Technological University Dublin

ARROW@TU Dublin

School of Mechanical and Design Engineering

Modelling and Simulation of a Biomass Gasification-solid Oxide Fuel Cell Combined Heat and Power Plant using Aspen Plus

Wayne Doherty
Technological University Dublin, wayne.doherty@tudublin.ie

Anthony Reynolds
Technological University Dublin, anthony.reynolds@tudublin.ie

David Kennedy
Technological University Dublin, david.kennedy@tudublin.ie

Follow this and additional works at: https://arrow.tudublin.ie/engschmeccon

Part of the Chemical Engineering Commons, and the Energy Systems Commons

Proceedings of ECOS 2009
Copyright © 2009 by ABCM

22nd International Conference on Efficiency, Cost, Optimization
Simulation and Environmental Impact of Energy Systems
August 31 – September 3, 2009, Foz do Iguaçu, Paraná, Brazil

MODELLING AND SIMULATION OF A BIOMASS GASIFICATION-SOLID OXIDE FUEL CELL COMBINED HEAT AND POWER PLANT USING ASPEN PLUS

Wayne Doherty, wayne.doherty@dit.ie
Anthony Reynolds, anthony.reynolds@dit.ie
Department of Mechanical Engineering, Dublin Institute of Technology, Bolton Street, Dublin 1, Ireland

David Kennedy, david.kennedy@dit.ie
Department of Mechanical Engineering, Dublin Institute of Technology, Bolton Street, Dublin 1, Ireland

Abstract. In this paper the operation and performance of a high temperature solid oxide fuel cell (SOFC) stack on biomass syn-gas from a demonstration biomass gasification combined heat and power (CHP) plant is investigated. The objective of this work is to develop a computer simulation model of a biomass-SOFC CHP system, flexible enough for use in industry, capable of predicting system performance under various operating conditions and using diverse fuels. The biomass gasifier is of the dual fluidised bed (DFB) type with steam as the gasifying agent and is operated at atmospheric pressure. The tubular SOFC configuration, developed by Siemens Power Generation Inc (SPGI), is selected. It is considered to be the most advanced design and is approaching commercialisation. The SOFC stack model, developed using the chemical process flowsheet simulator Aspen Plus, is of equilibrium type and is based on Gibbs free energy minimisation. The SOFC model performs heat and mass balances and considers the ohmic, activation and concentration losses for the voltage calculation. Data available in the literature on the SPGI SOFC operating on natural gas is used to validate the model. The system model predicts thermodynamic condition and composition of all internal flow streams, the heat generated by the SOFC stack, voltage (V), current (I) and efficiency. Operating parameters are varied over a wide range, parameters such as fuel utilisation factor (U_f), current density (j) and steam to carbon ratio (STCR) have significant influence. The results indicate that there must be a trade-off between voltage, efficiency and power with respect to j and the SOFC stack should be operated at low STCR and high U_f, within certain limits. SOFC stack operation on biomass syn-gas is compared to operation on natural gas and as expected there is a drop in performance, which is attributed to increased input fuel and air flow due to the lower quality of the fuel gas. The optimum realistic operating conditions with regard to SOFC stack performance are identified. High electrical efficiencies are predicted making these systems very attractive for CHP applications.

Keywords: biomass gasification, fuel cell, computer simulation, Gibbs free energy, model validation

1. INTRODUCTION

Biomass is among the most promising renewable energy sources in the context of both climate change mitigation and energy security. Energy is primarily recovered from biomass through combustion at low electrical efficiency, typically 20-25%. Biomass gasification coupled with advanced power generation technologies such as micro gas turbines and fuel cells offer much higher efficiencies. Reported electrical efficiencies (predicted) for biomass gasification-solid oxide fuel cell (SOFC) systems range from 23-50% (Seitarides *et al.* 2008). These systems offer highly efficient renewable energy and are modular in nature making them ideal for decentralised combined heat and power (CHP) applications and as a result have recently gained much attention (Pröll *et al.* 2004, Panopoulos *et al.* 2006, Cordiner *et al.* 2007, Sucipta *et al.* 2007, Suwanwarangkul *et al.* 2007, Fryda *et al.* 2008, Sucipta *et al.* 2008, Toonssen *et al.* 2008). Decentralised CHP is appropriate for biomass energy conversion systems as there may be major logistical problems regarding the availability of the fuel for large centralised plants.

Gasification occurs when a controlled amount of oxidant (pure oxygen (O_2), air, steam) is reacted at high temperatures with available carbon in biomass or other carbonaceous material within a gasifier, producing a combustible gas commonly known as syn-gas. Biomass syn-gas typically contains hydrogen (H_2), carbon monoxide (CO), methane (CH_4), carbon dioxide (CO_2), water (H_2O), nitrogen (N_2) and other components such as higher hydrocarbons. Air gasification produces a poor quality gas with regard to heating value, around 4-7 MJ/m^3 higher heating value (HHV), while O_2 and steam blown processes result in a syn-gas with a heating value in the range of 10-18 MJ/m^3 (HHV) (Schuster *et al.* 2001). Recently, Sucipta *et al.* (2007) found that biomass-SOFC systems achieved higher efficiencies when steam is used compared to pure O_2 or air. This is due to the higher heating value of the gas and the fact that the syn-gas is not diluted with N_2 and has high H_2 content. Atmospheric pressure fluidised bed gasification technology has been proven to operate effectively with many biomass fuels. These gasifiers have potential for scale-up from low MW to over 100 MW and possess high fuel flexibility, which is of utmost importance for biomass gasification plants as biomass fuels can be seasonal. Considering all of the above, the dual fluidised bed (DFB) steam gasification technology, also known as fast internally circulating fluidised bed (FICFB), was selected for this study. This technology is currently in operation at the Güssing demonstration CHP plant in Austria.

The SOFC is a highly efficient energy conversion device due to the fact that it converts the chemical energy contained in a fuel gas directly to electrical energy by means of electrochemical reactions. SOFCs are considered one of the most promising energy conversion devices since they can achieve very high electrical efficiencies with low emissions and good reliability (Calise *et al.* 2008). They can utilise a wide spectrum of fuels (natural gas, coal and biomass syn-gas) due to its high operating temperature, which also makes them suitable for integration with gas turbines and for cogeneration. The tubular SOFC configuration, developed by Siemens Power Generation Inc (SPGI) formerly Siemens-Westinghouse, is considered to be the most advanced and is approaching commercialisation, therefore it was selected for this study. Various models have been developed previously to simulate tubular SOFC performance, many of them for operation on humidified H_2 or natural gas (Bessette *et al.* 1995, Campanari, 2001, Campanari and Iora, 2004, Bharadwaj *et al.* 2005, Calì *et al.* 2007). A review of SOFC models, including those for planar and monolithic designs, can be found in the literature (Kakaç *et al.* 2007).

An advantage of the tubular SOFC is that it operates at a similar temperature to the biomass gasifier (800 – 1000 °C), making heat integration possible. Heat integration is attractive for steam gasification as it is an endothermic process. Recently, Athanasiou *et al.* (In Press) reported that the SOFC heat is sufficient to cover the requirements of the gasification process and syn-gas reforming with excess heat for a bottoming cycle. This will be investigated in a future study.

There is a need for SOFC models that are easily calibrated to match the continuous and rapid technological advances in the field. Also the models should have short computational times. In the present study the operation and performance of a tubular SOFC stack (SPGI design) on biomass syn-gas was investigated. The objective of this work was to develop a computer simulation model of a biomass-SOFC CHP system, flexible enough for use in industry, capable of predicting system performance under various operating conditions and using diverse fuels.

Aspen Plus, which is widely used in industry, was used to model the SOFC stack. There is no built in model that can represent a SOFC. A common approach is to develop a complete SOFC stack model in a programming language and link it to Aspen Plus as a subroutine (Zhang *et al.* 2005). The subroutine must incorporate complex phenomena such as chemical/electrochemical reactions and heat and mass transfer, making them difficult and time consuming to develop and use. This type of model would not achieve the objectives of this work. An alternative method proposed by Zhang *et al.* (2005), using existing Aspen Plus unit operation blocks with minimum requirements for linking of a subroutine was used. The equilibrium model, which is based on Gibbs free energy minimisation, performs heat and mass balances and considers the ohmic, activation and concentration losses for the voltage calculation. Equations reported by Song *et al.* (2005) were used to calculate ohmic loss, taking into account realistic electron/ion paths. Achenbach's semi-empirical correlations were implemented to determine the activation loss (Achenbach, 1994). Both ordinary and Knudsen diffusion were considered for the calculation of effective diffusion coefficients and the equations derived by Chan *et al.* (2001) were used for the calculation of the concentration loss.

2. TECHNOLOGY DESCRIPTION

2.1. Güssing biomass CHP plant

The Güssing biomass CHP plant has been in operation since 2001 and utilises 8 MW of wood chip fuel to produce 2 MW$_e$ of electricity (grid connected) by means of a gas engine and 4.5 MW$_{th}$ of heat (connected to the local district heating system). The biomass syn-gas is produced using a DFB steam gasifier. This type of gasifier operates with two separate zones, the combustion zone and the gasification zone. Residual char is combusted with air in the combustion zone and the heat is transferred to the gasification zone via circulating bed material. This heat drives the endothermic steam gasification reactions which produce the syn-gas. A more detailed description of the process can be found in the literature (Schuster *et al.* 2001, Pröll *et al.* 2004). Efforts are ongoing to get a SOFC stack installed for testing at the Güssing plant (Pröll, 2008). The following syn-gas composition was inputted to the SOFC stack model: 45.8% H_2, 21.6% CO, 10.0% CH_4, 21.2% CO_2, 1.4% N_2 (volume %, dry basis) and 25.7% H_2O (volume %, wet basis) (Pröll *et al.* 2004). This syn-gas composition is typical of the Güssing DFB gasifier operating at 850 °C with a steam/fuel ratio of 0.75 and after gas cleaning.

2.2. SPGI 100 kW CHP SOFC stack

The 100 kW AC CHP tubular SOFC stack developed by SPGI was selected and modelled. It was the first field unit to utilise the seal-less cathode supported cell (22 mm diameter, 150 cm active length, 834 cm^2 active area) and in stack reformers (George, 2000). This unit was operated on natural gas for over 20,000 hours in the Netherlands and Germany and provided 108 kW AC electricity and 85 kW of hot water for district heating at an AC efficiency of 47% (LHV) (Williams *et al.* 2004). This unit is currently installed at Gas Turbine Technologies in Torino, Italy and has been operated for a further 16,000 hours (Gariglio *et al.* In Press). It employs 1152 cells in 48 bundles of 24 cells each (Williams *et al.* 2004). The operation of this system is as follows:

Proceedings of ECOS 2009
Copyright © 2009 by ABCM

22nd International Conference on Efficiency, Cost, Optimization
Simulation and Environmental Impact of Energy Systems
August 31 – September 3, 2009, Foz do Iguaçu, Paraná, Brazil

The oxidant stream is fed via injector tubes, placed centrally in each SOFC, to the closed end of the cells. The oxidant then flows back through the annular space formed by the cathode surface and the injector tube to the open end. The oxidant is electrochemically reacted with the fuel supplied to the anode as it flows over the cathode surface. Cleaned fuel gas at sufficient pressure is supplied to the ejector where it is mixed with depleted fuel from the recirculation plenum. This anode recycle loop provides the steam and heat required for the steam reforming process. The mixed fuel then passes through the pre-reformers which convert the higher hydrocarbons and a small portion of the CH_4 adiabatically to H_2 and CO. The partially reformed fuel enters the internal reformers and using the heat generated by the exothermic electrochemical reactions occurring in the SOFC stack it is reformed further. The fuel then flows along the anode surface from the closed end to the open end, parallel to the direction of the oxidant flow and is electrochemically oxidised, generating electricity and increasing the temperature of both streams. A portion of the depleted fuel is recycled, the quantity of which depends on the required *STCR* and the remainder is reacted with the depleted oxidant in the combustion plenum. The generated heat serves to preheat the incoming oxidant stream in the injector tubes. The high temperature exhaust gas may then be utilised in a district heating system.

3. MODELLING

3.1. Aspen Plus flowsheet

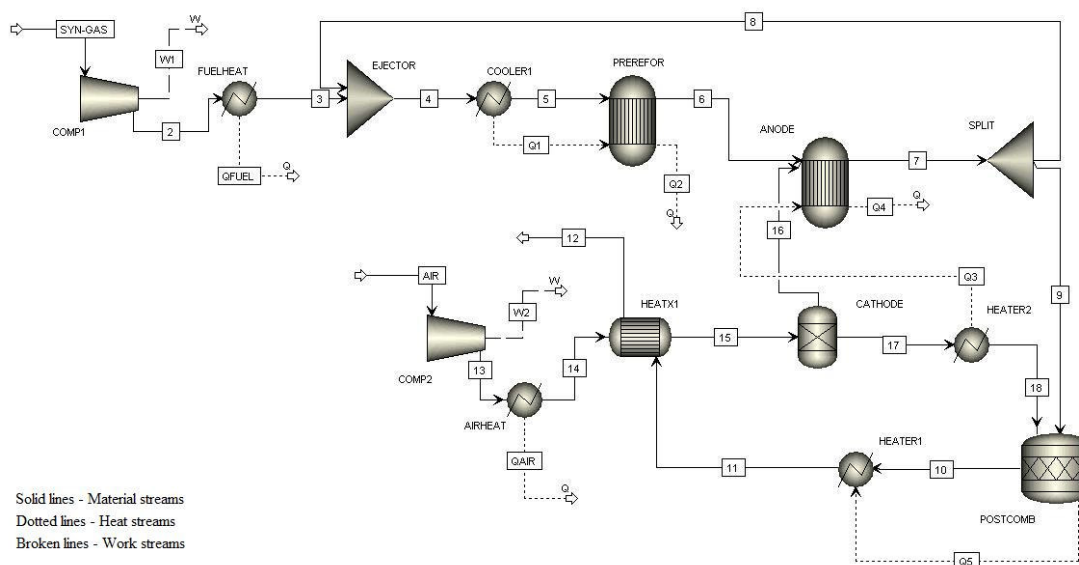Figure 1 depicts the Aspen Plus flowsheet of the SOFC stack.

Figure 1. SOFC stack model Aspen Plus flowsheet

3.2. Model description

3.2.1. Flowsheet description

With reference to Fig. 1, the stream 'SYN-GAS' is fed to the 'COMP1' block, simulating the fuel compressor. The discharge pressure was calculated by assuming a pressure ratio: $P_{fuel}/P_{SOFC} = 3$ (Campanari, 2001). The syn-gas stream composition and thermodynamic condition were inputted; its mole flow rate is set by a design spec and depends on the specified stack power (or for variable power a calculator block sets the mole flow depending on the specified *j*). The pressurised fuel is brought up to the fuel preheat temperature in the block 'FUELHEAT' and its exit stream enters the 'EJECTOR' block, where it is mixed with the recycled depleted fuel (stream 8). The pressure of the mixed stream (stream 4) is decreased back to slightly above atmospheric pressure (P_{SOFC}) and is directed to the 'COOLER1' block. The two blocks 'COOLER1' and 'PREREFOR' simulate the operation of the pre-reformers. The purpose of 'COOLER1' is to set the pre-reforming temperature. It is calculated by means of a design spec, which varies the temperature of 'COOLER1' until the net heat duty of 'PREREFOR' equals zero (adiabatic). As a result, the gas is cooled simulating the endothermicity of the steam reforming process. The following chemical reactions were specified in the 'PREREFOR' block:

Steam reforming: $C_nH_m + nH_2O \leftrightarrow (m/2 + n)H_2 + nCO$ (1)
Water-gas shift: $CO + H_2O \leftrightarrow CO_2 + H_2$ (2)

It was assumed that the reactions reach thermodynamic equilibrium at the pre-reforming temperature. The reader should note that it is possible that the reverse water-gas shift reaction is favoured at the high temperatures occurring in the SOFC stack. The pre-reformed fuel (stream 6) is fed to the 'ANODE' block, where the remaining CH_4 is reformed, CO is shifted and H_2 is oxidised. In a SOFC the following reactions occur:

Cathode half reaction: $0.5O_2 + 2e^- \rightarrow O^{2-}$ (3)
Anode half reaction: $H_2 + O^{2-} \rightarrow H_2O + 2e^-$ (4)
Overall reaction: $H_2 + 0.5O_2 \rightarrow H_2O$ (5)

The oxygen ion O^{2-} is the charge carrier in a SOFC. It is transported through the electrolyte to the anode side where it reacts with H_2 to produce electrons e^-. The transfer of ions cannot be modelled in Aspen Plus; therefore the overall reaction instead of the cell half reactions was used in the simulation. Although it is possible to directly oxidise CH_4 and CO in a SOFC at its high operating temperature, it is common to assume that the CH_4 is reformed and the CO is shifted to H_2 and therefore only H_2 participates in the electrochemical reaction. Reactions (1), (2) and (5) were specified in the 'ANODE' block and it was assumed that they reach thermodynamic equilibrium at the block temperature (T_{op} = 910 °C). The oxidant (stream 'AIR') is fed to the 'COMP2' block, the air compressor. Its discharge pressure was set as slightly above atmospheric pressure (P_{SOFC}). The air stream composition and thermodynamic condition were inputted. The molar flow rate is determined using a design spec that varies the air flow until the air utilisation factor U_a = 16.7% (Suwanwarangkul *et al.* 2007). The compressed air is brought up to the air preheat temperature in the block 'AIRHEAT' and its exit stream enters 'HEATX1' where it is preheated further by the hot combustion plenum products. The compressed and preheated air (stream 15) enters the 'CATHODE' block, whose function is to separate out the O_2 required for the electrochemical reaction ($nO_{2,consumed}$). The 'CATHODE' block O_2 split fraction is set by a calculator block using the following equations: $U_f = nH_{2,consumed}/nH_{2,in}$ where $nH_{2,consumed}$ is calculated, $nO_{2,consumed} = 0.5nH_{2,consumed}$ and O_2 split fraction = $nO_{2,consumed}/nO_{2,in}$. It is worth noting that the O_2 split fraction is equivalent to U_a. A typical value for U_f is 0.85. The $nH_{2,in}$ term is calculated as follows: $nH_{2,in} = nH_{2,syn-gas} + 1(nCO_{syn-gas}) + 4(nCH_{4,syn-gas}) + 7(nC_2H_{6,syn-gas}) + \dots$ where $nH_{2,syn-gas}$ represents the molar flow rate of H_2 contained in the stream 'SYN-GAS'; $1(nCO_{syn-gas})$ represents the molar flow rate of H_2 that could be produced from the CO contained in 'SYN-GAS'; $4(nCH_{4,syn-gas})$ represents the molar flow rate of H_2 that could be produced from the CH_4 in 'SYN-GAS' and the same applies to the higher hydrocarbons. Following the O_2 split calculation the required O_2 is directed to the 'ANODE' block (stream 16). The temperature of the depleted air (stream 17) must be increased to the stack operating temperature (T_{op}). The heat needed to do this is supplied by the electrochemical reaction and this process was simulated by taking a heat stream (Q3) from 'HEATER2' to 'ANODE'. The temperature of the 'HEATER2' block was specified as 910 °C (T_{op}). The depleted fuel (stream 7) enters the block 'SPLIT', whose function is to split the stream into a recycle (stream 8) and a stream directed to the combustion plenum. The split fraction of the block is set using a design spec where it is determined by a specified *STCR*, defined as the molar ratio of steam to combustible carbon, a typical value being 2.5. Excess steam as well as increasing the concentration of H_2 and CO_2 inhibits the formation of carbon. Carbon deposition not only represents a loss in the system but results in deactivation of catalysts and decreases the activity of the anode by clogging the active sites. The depleted fuel and oxidant are fed to 'POSTCOMB' where complete combustion of the remaining fuel occurs. The following combustion reactions, assumed to reach completion, were specified:

H_2 combustion: $H_2 + 0.5O_2 \rightarrow H_2O$ (6)
CO combustion: $CO + 0.5O_2 \rightarrow CO_2$ (7)
CH_4 combustion: $CH_4 + 2O_2 \rightarrow CO_2 + 2H_2O$ (8)

The heat generated by the reactions is calculated and is put into the heat stream Q5, which is fed to the block 'HEATER1', whose function is to calculate and set the combustion products temperature. Finally, the high temperature combustion products (stream 11) exchange heat with and serve to preheat the incoming air in the 'HEATX1' block. The temperature of the SOFC stack exhaust (stream 12), which may be utilised in a district heating system, is also determined.

3.2.2. Voltage calculation

The voltage was calculated by first applying the widely known Nernst equation, Eq. (9) Tab. 1, to determine the reversible Nernst voltage (V_N) and then subtracting the various losses, including ohmic, activation and concentration losses. In Eq. (9) $\Delta \overline{g}_f$ is the molar Gibbs free energy of formation (J/mol) at standard pressure (1 bar), 2 represents the number of electrons produced per mole of H_2 fuel reacted, F is the Faraday constant (96485 C/mol), T_{avg} is the average temperature between the SOFC inlet and outlet streams (K), R_g is the molar gas constant and was taken as 8.314 J/mol

Proceedings of ECOS 2009
Copyright © 2009 by ABCM

22nd International Conference on Efficiency, Cost, Optimization
Simulation and Environmental Impact of Energy Systems
August 31 – September 3, 2009, Foz do Iguaçu, Paraná, Brazil

K and P_i is the partial pressure (in bar) of gaseous component i. The partial pressures were taken as average values of the anode and cathode inlet and outlet streams. The gas composition changes along the length of the SOFC anode and cathode and thus the Nernst voltage and current varies with axial direction; however the 0-D model developed here only predicts the outlet gas composition, which was the reason for using the average values. For 2-D or 3-D models average values would not be used as the SOFC would be divided into sections and the Nernst voltage calculated for each section using the local gas composition.

Table 1. Voltage calculation equations

Reversible Nernst voltage		
Nernst equation	$V_N = -\dfrac{\Delta \overline{g}_f}{2 \cdot F} + \dfrac{R_g \cdot T_{avg}}{2 \cdot F} \ln \dfrac{P_{H_2} \cdot P_{O_2}^{\,0.5}}{P_{H_2O}}$	(9)
Ohmic loss		
Anode	$V_{Ohm\_A} = \dfrac{j \cdot \rho_A (A \cdot \pi \cdot D_m)^2}{8 \cdot t_A}$	(10)
Cathode	$V_{Ohm\_C} = \dfrac{j \cdot \rho_C (\pi \cdot D_m)^2}{8 \cdot t_C} \cdot A[A + 2(1 - A - B)]$	(11)
Electrolyte	$V_{Ohm\_E} = j \cdot \rho_E \cdot t_E$	(12)
Interconnection	$V_{Ohm\_Int} = j \cdot \rho_{Int} (\pi \cdot D_m) \dfrac{t_{Int}}{w_{Int}}$	(13)
Activation loss		
Anode	$\dfrac{1}{R_{Act\_A}} = \dfrac{2 \cdot F}{R_g \cdot T_{op}} \cdot k_A \left(\dfrac{P_{H_2}}{P^0}\right)^m \exp\left(\dfrac{-E_A}{R_g \cdot T_{op}}\right)$	(14)
Cathode	$\dfrac{1}{R_{Act\_C}} = \dfrac{4 \cdot F}{R_g \cdot T_{op}} \cdot k_C \left(\dfrac{P_{O_2}}{P^0}\right)^m \exp\left(\dfrac{-E_C}{R_g \cdot T_{op}}\right)$	(15)
Concentration loss		
Anode	$V_{Conc\_A} = -\dfrac{R_g \cdot T_{op}}{2 \cdot F} \ln\left[\dfrac{1 - (R_g \cdot T_{op}/2 \cdot F)(t_A/D_{An(eff)} \cdot y^0_{H_2} \cdot P_{SOFC})j}{1 + (R_g \cdot T_{op}/2 \cdot F)(t_A/D_{An(eff)} \cdot y^0_{H_2O} \cdot P_{SOFC})j}\right]$	(16)
Cathode	$V_{Conc\_C} = -\dfrac{R_g \cdot T_{op}}{4 \cdot F} \ln\left[\dfrac{(P_{SOFC}/\delta_{O_2}) - ((P_{SOFC}/\delta_{O_2}) - y^0_{O_2} P_{SOFC}) \exp[(R_g \cdot T_{op}/4 \cdot F)(\delta_{O_2} \cdot t_C / D_{Cat(eff)} \cdot P_{SOFC})j]}{y^0_{O_2} \cdot P_{SOFC}}\right]$	(17)
Actual voltage		
	$V = V_N - (V_{Ohm} + V_{Act} + V_{Conc})$	(18)

The ohmic loss, which is the voltage loss due to the resistance to electron flow through both electrodes and the interconnection and the resistance to ion flow through the electrolyte, was calculated using Eq. (10) – (13). These equations developed by Song *et al.* (2005) take into account realistic electron/ion paths in a tubular SOFC. They assumed uniform current density in the circumferential direction and uniform ionic flux in the electrolyte in the radial direction. The angle related to the extent of electrical contact is $A\pi$ radians while the angle $B\pi$ radians is related to the interconnection. The equations were developed using Ohm's law: $V_{Ohm\_i} = IR_i$ and the resistivity equation: $R_i = \rho_i(l_i/A_i)$, where ρ_i is the material resistivity (Ω m), l_i is the current flow length (m) and A_i is the area through which the current flows (m^2). The resistivity terms were determined using the temperature dependent relations proposed by Bessette *et al.* (1995), given in Tab. 2. Other terms that appear in Eq. (10) – (13) include D_m, which is the mean diameter of a cell (m), calculated from the geometry parameters given in Tab. 2, the cell component thickness t_i (m) and the interconnection width w_{Int} (m). Uniform axial voltage is assumed and also no current transport in the axial direction. The ohmic loss is especially important for tubular SOFCs as it is the dominant loss due to long current flow paths.

Table 2. Input parameters

Geometry parameters (Campanari and Iora, 2004, Williams *et al.* 2004)	
Cell length (m)	1.5
Cell outer diameter (m)	0.022
Anode thickness t_A (m)	0.0001
Cathode thickness t_C (m)	0.0022
Electrolyte thickness t_E (m)	0.00004
Interconnection thickness t_{Int} (m)	0.000085
Interconnection width w_{Int} (m)	0.009
Material properties	
Anode resistivity ρ_A (Ω m) (Bessette *et al.* 1995)	$2.98 \times 10^{-5} \exp(-1392/T_{op})$
Cathode resistivity ρ_C (Ω m) (Bessette *et al.* 1995)	$8.114 \times 10^{-5} \exp(600/T_{op})$
Electrolyte resistivity ρ_E (Ω m) (Bessette *et al.* 1995)	$2.94 \times 10^{-5} \exp(10350/T_{op})$
Interconnection resistivity ρ_{Int} (Ω m) (Campanari and Iora, 2004)	0.025
Ohmic loss (Song *et al.* 2005)	
A / B	0.804 / 0.13
Activation loss (Achenbach, 1994)	
Pre-exponential factor k_A / k_C (A/m^2)	2.13×10^8 / 1.49×10^{10}

Slope m	0.25
Activation energy E_A / E_C (J/mol)	110000 / 160000
Concentration loss	
Electrode pore radius r (m) (Chan *et al.* 2001)	5×10^{-7}
Electrode porosity ε / tortuosity ξ (Calise *et al.* 2008)	0.5 / 5.9

The activation loss due to slow or sluggish kinetics of the electrochemical reaction taking place on the electrodes was determined using the semi-empirical correlations proposed by Achenbach, (1994) (14) and (15). It is the voltage lost as a result of the energy barrier that must be overcome by the reacting species. In Eq. (14) and (15) the R_{Act_i} terms represent specific resistance (Ω m^2) at both anode and cathode. The activation voltage loss V_{Act_i} was evaluated by multiplying the specific resistance terms by j (A/m^2). The pre-exponential factors k_i, determined experimentally are listed in Tab. 2. The partial pressures P_i (bar) were taken as average values of the anode and cathode inlet and outlet streams. P^0 is a reference pressure and was taken as 1 bar; the influence of partial pressure is accounted for by the slope m. The E_i terms are activation energies and are listed in Tab. 2. The activation voltage loss is less significant in SOFCs compared to other fuel cells due to the high operating temperature.

The concentration loss due to mass transfer limitations in the porous electrodes was modelled using Eq. (16) and (17), which were derived by Chan *et al.* (2001). Diffusion transport in the electrodes (gases in pores) was considered with convection in the gas channel neglected. The diffusion driving force is the difference in concentration of reactants and products between the reacting sites and the bulk flow, caused by current being drawn from the cell. Equations (16) and (17) were derived using Fick's law of diffusion and both ordinary and Knudsen diffusion were considered. Ordinary diffusion occurs when the pore diameter of the material is large in comparison to the mean free path of the gas molecules, whereas Knudsen diffusion occurs when the pores are small (Chan *et al.* 2001). For the Knudsen type the gas molecules are impeded due to frequent collisions with the pore walls. Both types of diffusion were accounted for by calculating effective diffusion coefficients for the anode and cathode. The following equation was used to determine the Knudsen diffusion coefficients for the anode and cathode gases: $D_{A,K} = 97r(T_{op}/M_A)^{0.5}$ (m^2/s) where subscript A represents the gaseous component (H_2, H_2O, O_2 or N_2), r is the electrode pore radius (m) and M_A is the molecular weight (kg/kmol) of the gaseous component. The effective Knudsen diffusion coefficient is given by: $D_{A,K(eff)} = D_{A,K}(\varepsilon/\xi)$ where ε is porosity and ξ is tortuosity of the electrodes. The following semi-empirical correlation, based on the kinetic theory of gases and proposed by Fuller *et al.* (1966), was used to calculate the ordinary binary diffusion coefficient for both anode and cathode: $D_{AB} = 1 \times 10^{-7} T_{op}^{1.75}(1/M_A + 1/M_B)^{0.5}/P(v_A^{1/3} + v_B^{1/3})^2$ (m^2/s) where subscripts A and B represent the gaseous components that make up the binary gas mixture (H_2-H_2O at the anode and O_2-N_2 at the cathode), P is pressure in atmospheres and v_i is the Fuller diffusion volume, taken as 7.07, 12.7, 16.6 and 17.9 for H_2, H_2O, O_2 and N_2 respectively (Fuller *et al.* 1966). Similar to the case of Knudsen diffusion, the effective ordinary diffusion coefficient is given by: $D_{AB(eff)} = D_{AB}(\varepsilon/\xi)$. The overall effective diffusion coefficient for each gas was then calculated using: $1/D_{A(eff)} = 1/D_{AB(eff)} + 1/D_{A,K(eff)}$. Finally, the anode and cathode diffusion coefficients were calculated: $D_{An(eff)} = (P_{H2O}/P_{SOFC})D_{H2(eff)} + (P_{H2}/P_{SOFC})D_{H2O(eff)}$ and $D_{Cat(eff)} = D_{O2(eff)}$. δ_{O2} in Eq. (17) was found using: $\delta_{O2} = D_{O2,K(eff)}/(D_{O2,K(eff)} + D_{O2N2(eff)})$. The y^0_i terms are the gas molar fractions in the bulk flow, taken as the average values of the anode and cathode inlet and outlet streams. This loss is low unless the current density is high and the fuel and air concentrations are low, caused by high utilisations (U_f and U_a). Under these conditions the limiting current may be reached reducing the fuel cell voltage to very low levels.

Finally, the actual voltage V was calculated using Eq. (18), which is simply the Nernst voltage less the sum of the voltage losses. The calculations described above are carried out using a design spec, which varies the input fuel flow until the SOFC stack DC power ($P_{el,DC} = VI$) equals a specified value (base case: 120 kW). However, for known current, as was the case for the current density sensitivity analysis (section 4.2.1.), a calculator block determines and sets the input fuel flow using: $nH_{2,in}$ (kmol/h) = $(I/2FU_f)(3600/1000)$ and $nFuel_{in}$ (kmol/h) = $nH_{2,in}/(yH_2 + yCO + 4yCH_4 + 7yC_2H_6 + 10yC_3H_8 + 13yC_4H_{10})$ where y_i is the molar fraction of gaseous component i, then V and $P_{el,DC}$ are calculated. In both cases, the gross and net AC efficiencies (LHV basis) are determined. The gross AC efficiency is defined as: $\eta_{el,gross} = P_{el,AC}/(nFuel_{in}LHV_{fuel})$ where $P_{el,AC}$ is the SOFC stack AC power (kW), $nFuel_{in}$ is the molar flow of input fuel (kmol/s) and LHV_{fuel} is the lower heating value of the input fuel (kJ/kmol). The net AC efficiency is defined as: $\eta_{el,net} = (P_{el,AC} - P_{comp})/(nFuel_{in}LHV_{fuel})$ where P_{comp} is the electrical power requirement of the fuel and air compressors (kW).

4. RESULTS

4.1. Model validation

The developed model was validated against published data for the SPGI 100 kW CHP SOFC stack operating on natural gas. The model inputs were as follows (Campanari, 2001, Zhang *et al.* 2005):

- Natural gas composition (mole %): CH_4 81.3%, C_2H_6 2.9%, C_3H_8 0.4%, C_4H_{10} 0.2%, N_2 14.3%, CO_2 0.9%.
- Operating pressure (P_{SOFC}): 1.08 atm.

Proceedings of ECOS 2009
Copyright © 2009 by ABCM

22nd International Conference on Efficiency, Cost, Optimization
Simulation and Environmental Impact of Energy Systems
August 31 – September 3, 2009, Foz do Iguaçu, Paraná, Brazil

- Ejector pressure ratio (P_{fuel}/P_{SOFC}): 3.
- DC power ($P_{el,DC}$): 120 kW.
- Active area (S): 96.0768 m^2 (1152 cells).
- Operating / anode and cathode exhaust temperature (T_{op}): 910 °C.
- Input air / fuel temperature: 630 / 200 °C.
- U_f / U_a / STCR: 85% / 19% / 1.8.
- Cold and hot stream temperature difference (SOFC recuperator 'HEATX1'): 10 °C.
- DC to AC inverter efficiency: 92%.

Table 3. SOFC model validation

	Literature (Zhang *et al.* 2005)	**Model results**
Voltage (V)	0.7	0.683
Current density (A/m^2)	1780	1828.6
Air utilisation factor (%)	19	19
Pre-reforming temperature (°C)	536	535.1
Pre-reformer CH$_4$ conversion (%)	25.9	25
Pre-reformer higher hydrocarbon conversion (%)	100	100
Anode inlet gas composition (mole %)	H$_2$ 27, CO 5.6, CH$_4$ 10.1, H$_2$O 27.9, CO$_2$ 23.1, N$_2$ 6.2	H$_2$ 26.9, CO 5.6, CH$_4$ 10.4, H$_2$O 27.8, CO$_2$ 23.1, N$_2$ 6.2
Anode exhaust gas composition (mole %)	H$_2$ 11.6, CO 7.4, H$_2$O 50.9, CO$_2$ 24.9, N$_2$ 5.1	H$_2$ 11.6, CO 7.4, H$_2$O 50.9, CO$_2$ 24.9, N$_2$ 5.1
Cathode inlet temperature (°C)	821.32	823.7
Cathode exhaust gas composition (mole %)	O$_2$ 17.7, N$_2$ 82.3	O$_2$ 17.7, N$_2$ 82.3
Combustion products temperature (°C)	1012.35	1012.3
Stack exhaust temperature (°C)	833.85	833.7
Stack exhaust gas composition (mole %)	H$_2$O 4.5, CO$_2$ 2.3, O$_2$ 15.9, N$_2$ 77.3	H$_2$O 4.5, CO$_2$ 2.3, O$_2$ 15.9, N$_2$ 77.3
Gross AC efficiency (LHV) (%)	52	51.28
Net AC efficiency (LHV) (%)	-	49.15

The model results are in good agreement with published work (please refer to Tab. 3). There is only a slight difference for voltage, current density and efficiency. The reader should note that Zhang *et al.* (2005) used a very different method for calculating the voltage to the one applied in this work. They used semi-empirical correlations developed using a reference polarisation curve. For comparison, Campanari, (2001) reports a voltage and current density of 0.69 V and 1800 A/m^2 and a net AC efficiency of 48.5%. These results compare well with this work.

4.2. Sensitivity analyses

The model described was used to perform sensitivity analyses. The effects of varying *j*, STCR and U_f on SOFC stack performance were investigated. During the sensitivity analyses the model input base case data was kept the same as for model validation with the following exceptions: fuel input (Güssing biomass syn-gas) composition as given in section 2.1., input fuel temperature = 300 °C, U_a = 16.7% and STCR = 2.5.

Comparing SOFC stack operation on biomass syn-gas to natural gas (see section 4.1.) at *j* = 1828.6 A/m^2, voltage was observed to decrease by 14 mV to 0.669 V, gross efficiency reduced 8.28% to 43%, net efficiency reduced 11.63% to 37.52% and DC power decreased 2.43 kW to 117.57 kW. The relatively large drop in efficiency is attributed to increased input fuel and air flow, which is due to the lower quality of the fuel gas. Even with this performance decrease the efficiency achieved is much higher than traditional biomass systems, making this technology very promising. For a required DC power of 120 kW using base case data and biomass syn-gas fuel the SOFC stack performance was as follows: *j* = 1887 A/m^2, *V* = 0.662 V, $\eta_{el,gross}$ = 42.53% and $\eta_{el,net}$ = 37.04%. These have been identified as the optimum realistic operating conditions with regard to stack performance.

4.2.1. Effect of current density

In this case the current was an input and the voltage and DC power were calculated. Figure 2 shows the effects of varying *j* on the system. Increasing *j* decreases both efficiency and voltage but increases power. Voltage is lowered as a result of higher voltage losses (ohmic, activation and concentration) and efficiency decreases due to increased input fuel flow. Increased *j* requires the input air flow to increase to provide the O$_2$ ions for the electrochemical reaction, which in turn increases the air compressor parasitic power and lowers the efficiency. It is desirable with regard to operating costs, to operate the SOFC stack at a high voltage and efficiency; however it is also desirable with regard to capital costs, to operate the SOFC stack at high power (less SOFCs needed). Therefore there must be a trade-off between voltage, efficiency and power. A typical operating *j* range is 1800 – 2000 A/m^2, corresponding to a cell voltage of 0.673 – 0.647 V, $\eta_{el,gross}$ = 43.2 – 41.6%, $\eta_{el,net}$ = 37.8 – 36.1% and $P_{el,DC}$ = 116.36 – 124.41 kW.
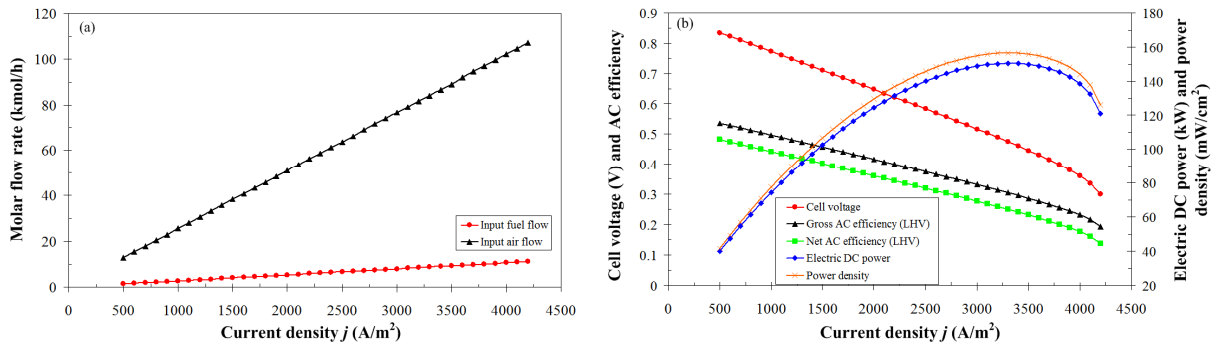
Figure 2. Effect of current density on (a) input fuel and air flow and (b) voltage, efficiency and power

4.2.2. Effect of steam to carbon ratio

The effects of varying *STCR* are displayed in Fig. 3. *STCR* has a substantial impact on the pre-reformer, the inlet temperature increases from 408 to 729 °C over the *STCR* range, which in turn causes the anode temperature to rise (558 to 633 °C) and results in greater CH_4 conversion (0 to 92.2%). The high temperature and greater amount of steam available promotes the steam reforming of CH_4. The pre-reformer inlet temperature increases with *STCR* due to the recirculation of more high temperature depleted fuel, which is advantageous as the anode inlet gas will be closer to the SOFC operating temperature thus reducing the stack thermal gradient. On the other hand the greater flow into the pre-reformer means a larger pre-reformer is required and thus increased capital costs. Increasing *STCR* has a negative impact on voltage and efficiency and increases *j*, this is due to the change in anode temperature and gaseous component partial pressures, which decreases the Nernst voltage and increases the voltage losses. It is therefore desirable to operate the stack at low *STCR*. However the *STCR* must be high enough to ensure no carbon formation on the anode. Considering the findings above it is recommended to operate the SOFC stack at a *STCR* as low as possible but high enough as to ensure no carbon formation.
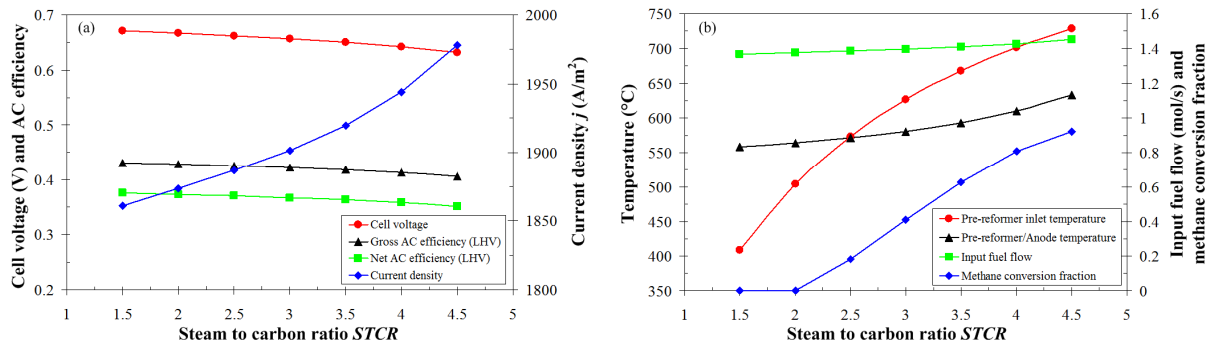

Figure 3. Effect of steam to carbon ratio on (a) voltage, efficiency and current density and (b) pre-reformer inlet temperature, pre-reformer/anode temperature, input fuel flow and methane conversion fraction

4.2.3. Effect of fuel utilisation factor

Figure 4 depicts the influence of U_f on SOFC stack performance. The cell voltage decreases with U_f as the fuel is more depleted, which increases the voltage losses. The current density increases due to the higher amount of H_2 consumed on the anode ($I = 2Fn H_{2,consumed}$). The input fuel required to achieve the DC power of 120 kW decreases with U_f because more of the energy contained in the fuel is converted to electricity and less to heat in the combustion plenum due to the higher H_2 consumed. Efficiency increases as a result of the reduced fuel input. The amount of recirculated fuel decreases with U_f as less fuel needs to be recirculated to meet the specified *STCR* due to the increased H_2O content in the depleted fuel. As a result of less high temperature depleted fuel being recirculated the pre-reformer/anode temperature drops and thus the CH_4 conversion fraction is lowered. At low U_f more of the fuel input is combusted, which results in a higher combustion temperature and therefore increased cathode and stack exhaust temperatures. As U_f increases more of the fuel H_2 is converted to electricity meaning less is available to the combustion plenum thus lowering the combustion temperature and therefore the cathode and stack exhaust temperatures. Considering the findings above it is recommended to operate the SOFC stack at high fuel utilisation but below the level where the

Proceedings of ECOS 2009
Copyright © 2009 by ABCM

22nd International Conference on Efficiency, Cost, Optimization
Simulation and Environmental Impact of Energy Systems
August 31 – September 3, 2009, Foz do Iguaçu, Paraná, Brazil

concentration loss increases to a very high degree. A typical U_f is 0.85. However if the SOFC stack was thermally integrated with a gasifier then the level of heat available in the exhaust would need to be considered. In this case a low U_f would have to be used (typically 0.7) to ensure that sufficient heat was available to the gasifier.
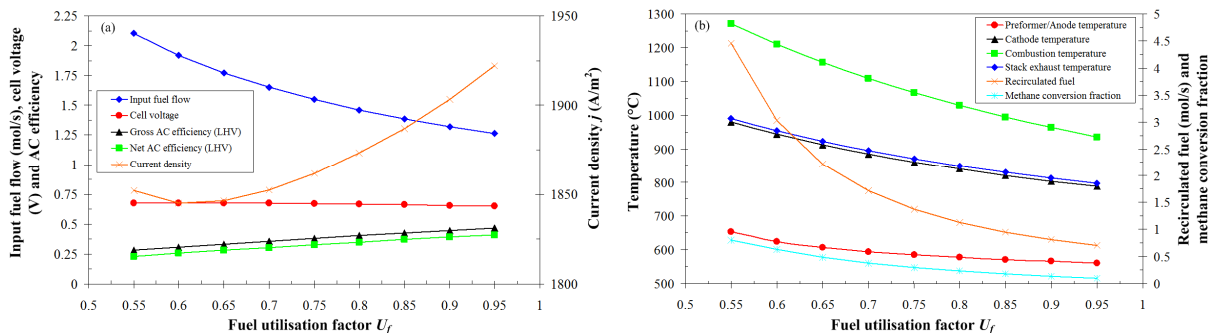

Figure 4. Effect of fuel utilisation factor on (a) voltage, efficiency, input fuel flow and current density and (b) pre-reformer/anode temperature, cathode temperature, combustion temperature, stack exhaust temperature, recirculated fuel and methane conversion fraction

5. CONCLUSIONS

A computer simulation model of the SPGI 100 kW AC CHP tubular SOFC stack was developed using Aspen Plus. The objective of the work, which was to develop a computer simulation model flexible enough for use in industry and capable of predicting system performance under various operating conditions and using diverse fuels, was achieved. The objective was achieved by developing a model using existing Aspen Plus unit operation blocks with minimum requirements for linking of a subroutine thus reducing the model complexity and ensuring a short computational time. The model was validated against published data for the SPGI 100 kW SOFC stack operating on natural gas. Sensitivity analyses were carried out in order to give insight into the influence of the main variables on the system. The effects of varying current density j, steam to carbon ratio $STCR$ and fuel utilisation factor U_f on SOFC stack performance were investigated for the stack operating on biomass syn-gas (from Güssing DFB steam gasifier), the results of which revealed the following:

- There must be a trade-off between voltage, efficiency and power with respect to j. For j = 1800 to 2000 A/m^2, cell voltage = 0.673 to 0.647 V, DC power = 116.36 to 124.41 kW and electrical efficiency = 43.2 to 41.6% (gross) and 37.8 to 36.1% (net).
- The SOFC stack should be operated at a low $STCR$ that is high enough to inhibit carbon formation.
- The SOFC stack should be operated at high U_f but below the level where the concentration loss increases to a very high degree.
- SOFC stack operation on biomass syn-gas compared to natural gas: voltage decreases by 14 mV to 0.669 V, gross efficiency reduced 8.28% to 43%, net efficiency reduced 11.63% to 37.52% and DC power decreased 2.43 kW to 117.57 kW. The drop in efficiency is attributed to increased input fuel and air flow due to the lower quality of the fuel gas. Even with this performance decrease the efficiency achieved is much higher than traditional biomass systems, making this technology very promising.
- The optimum realistic operating conditions with regard to stack performance were identified: $STCR$ = 2.5, U_f = 0.85, DC power = 120 kW, j = 1887 A/m^2, cell voltage = 0.662 V and electrical efficiency = 42.53% (gross) and 37.04% (net).

Future work includes integration of the SOFC stack model with a biomass gasifier model where issues such as thermal integration and gas cleaning (tar elimination etc.) will be addressed.

REFERENCES

Achenbach, E., 1994, "Three-dimensional and time-dependent simulation of a planar solid oxide fuel cell stack", Journal of Power Sources, 49, 1-3, 333-348.
Athanasiou, C., Vakouftsi, E., Coutelieris, F.A., Marnellos, G. and Zabaniotou, A., "Efficiencies of olive kernel gasification combined cycle with solid oxide fuel cells (SOFCs)", Chemical Engineering Journal, In Press, Corrected Proof.

Bessette, N.F., Wepfer, W.J. and Winnick, J., 1995, "A mathematical model of a solid oxide fuel cell", Journal of the Electrochemical Society, 142, 11, 3792-3800.

Bharadwaj, A., Archer, D.H. and Rubin, E.S., 2005, "Modeling the performance of a tubular solid oxide fuel cell", Journal of Fuel Cell Science and Technology, 2, 38.

Calì, M., Santarelli, M.G.L. and Leone, P., 2007, "Design of experiments for fitting regression models on the tubular SOFC : Screening test, response surface analysis and optimization", International Journal of Hydrogen Energy, 32, 3, 343-358.

Calise, F., d'Accadia, M.D., Palombo, A. and Vanoli, L., 2008, "One-dimensional model of a tubular solid oxide fuel cell", Journal of Fuel Cell Science and Technology, 5, 021014-1-15.

Campanari, S., 2001, "Thermodynamic model and parametric analysis of a tubular SOFC module", Journal of Power Sources, 92, 1-2, 26-34.

Campanari, S. and Iora, P., 2004, "Definition and sensitivity analysis of a finite volume SOFC model for a tubular cell geometry", Journal of Power Sources, 132, 1-2, 113-126.

Chan, S.H., Khor, K.A. and Xia, Z.T., 2001, "A complete polarization model of a solid oxide fuel cell and its sensitivity to the change of cell component thickness", Journal of Power Sources, 93, 1-2, 130-140.

Cordiner, S., Feola, M., Mulone, V. and Romanelli, F., 2007, "Analysis of a SOFC energy generation system fuelled with biomass reformate", Applied Thermal Engineering, 27, 4, 738-747.

Fryda, L., Panopoulos, K.D. and Kakaras, E., 2008, "Integrated CHP with autothermal biomass gasification and SOFC-MGT", Energy Conversion and Management, 49, 2, 281-290.

Fuller, E.N., Schettler, P.D. and Giddings, J.C., 1966, "A new method for prediction of binary gas-phase diffusion coefficients", Industrial and Engineering Chemistry, 58, 5, 19-27.

Gariglio, M., De Benedictis, F., Santarelli, M., Calì, M. and Orsello, G., "Experimental activity on two tubular solid oxide fuel cell cogeneration plants in a real industrial environment", International Journal of Hydrogen Energy, In Press, Corrected Proof.

George, R.A., 2000, "Status of tubular SOFC field unit demonstrations", Journal of Power Sources, 86, 1-2, 134-139.

Kakaç, S., Pramuanjaroenkij, A. and Zhou, X.Y., 2007, "A review of numerical modeling of solid oxide fuel cells", International Journal of Hydrogen Energy, 32, 7, 761-786.

Panopoulos, K.D., Fryda, L.E., Karl, J., Poulou, S. and Kakaras, E., 2006, "High temperature solid oxide fuel cell integrated with novel allothermal biomass gasification: Part I: Modelling and feasibility study", Journal of Power Sources, 159, 1, 570-585.

Pröll, T., 2008, Private Communication, Vienna University of Technology, Vienna, Austria.

Pröll, T., Rauch, R., Aichernig, C. and Hofbauer, H., 2004, "Coupling of biomass steam gasification and an SOFC-gas turbine hybrid system for highly efficient electricity generation", ASME Turbo Expo: Power for Land, Sea, and Air, Vienna, Austria.

Schuster, G., Löffler, G., Weigl, K. and Hofbauer, H., 2001, "Biomass steam gasification - an extensive parametric modeling study", Bioresource Technology, 77, 1, 71-79.

Seitarides, T., Athanasiou, C. and Zabaniotou, A., 2008, "Modular biomass gasification-based solid oxide fuel cells (SOFC) for sustainable development", Renewable and Sustainable Energy Reviews, 12, 5, 1251-1276.

Song, T.W., Sohn, J.L., Kim, J.H., Kim, T.S., Ro, S.T. and Suzuki, K., 2005, "Performance analysis of a tubular solid oxide fuel cell/micro gas turbine hybrid power system based on a quasi-two dimensional model", Journal of Power Sources, 142, 1-2, 30-42.

Sucipta, M., Kimijima, S., Song, T.W. and Suzuki, K., 2008, "Biomass solid oxide fuel cell-microgas turbine hybrid system: Effect of fuel composition", Journal of Fuel Cell Science and Technology, 5, 041006-1-8.

Sucipta, M., Kimijima, S. and Suzuki, K., 2007, "Performance analysis of the SOFC-MGT hybrid system with gasified biomass fuel", Journal of Power Sources, 174, 1, 124-135.

Suwanwarangkul, R., Croiset, E., Pritzker, M.D., Fowler, M.W., Douglas, P.L. and Entchev, E., 2007, "Modelling of a cathode-supported tubular solid oxide fuel cell operating with biomass-derived synthesis gas", Journal of Power Sources, 166, 2, 386-399.

Toonssen, R., Woudstra, N. and Verkooijen, A.H.M., 2008, "Reference system for a power plant based on biomass gasification and SOFC", 8th European Solid Oxide Fuel Cell Forum, Lucerne, Switzerland.

Williams, M.C., Strakey, J.P. and Singhal, S.C., 2004, "U.S. distributed generation fuel cell program", Journal of Power Sources, 131, 1-2, 79-85.

Zhang, W., Croiset, E., Douglas, P.L., Fowler, M.W. and Entchev, E., 2005, "Simulation of a tubular solid oxide fuel cell stack using AspenPlusTM unit operation models", Energy Conversion and Management, 46, 2, 181-196.

RESPONSIBILITY NOTICE

The authors are the only persons responsible for the printed material included in this paper.